CARBON 63 (2013) 454–459

Available at www.sciencedirect.com

SciVerse ScienceDirect

journal homepage: www.elsevier.com/locate/carbon

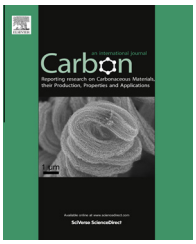

Reduction of graphene oxide films on Al foil for hybrid transparent conductive film applications

Sergio H. Domingues [a,b], *Iskandar N. Kholmanov* [a,c], *TaeYoung Kim* [a], *JinYoung Kim* [a], *Cheng Tan* [a], *Harry Chou* [a], *Zeineb A. Alieva* [a], *Richard Piner* [a], *Aldo J.G. Zarbin* [b], *Rodney S. Ruoff* [a,*]

[a] *Department of Mechanical Engineering and the Materials Science and Engineering Program, The University of Texas at Austin, 1 University Station C2200, Austin, TX 78712, USA*

[b] *Department of Chemistry, Universidade Federal do Paraná, CP 19081, CEP 81531-990 Curitiba, PR, Brazil*

[c] *CNR-IDASC Sensor Lab Department of Chemistry and Physics, University of Brescia, via Valotti, 9, Brescia 25133, Italy*

ARTICLE INFO

Article history:
Received 29 May 2013
Accepted 3 July 2013
Available online 8 July 2013

ABSTRACT

We report the reduction of graphene oxide (G-O) films on Al foil using hydrogen as a reducing agent generated during the etching of Al foil in an aqueous solution of hydrochloric acid (HCl). Complete etching of the Al substrate results in simultaneous reduction and a free standing film composed of stacked and overlapped reduced graphene oxide (RG-O) platelets. Generation of hydrogen at the G-O/Al interface increases the reduction efficiency of this method that is demonstrated in better electrical conductivity of the obtained films compared to the RG-O films reduced by the similar method but using remote Al foil in HCl solution and hydrazine reduced RG-O films. By transferring the free standing RG-O films onto Ag NW films, hybrid transparent conductive films (TCFs) with opto-electrical properties comparable to that of ITO films were obtained.

1. Introduction

Graphene oxide (G-O) properties can be easily tailored, making it of interest for a wide range of potential applications [1–6]. Primarily, the reduction of G-O can change its chemical structure, remove the majority of oxygen containing functional groups and dramatically alter its electronic, optical, thermal, and chemical properties [7–10]. Many chemicals including hydrazine [11], sodium borohydride [12], hydroquinone [13], dimethylhydrazine [1], hydriodic acid [14] and ascorbic acid [15] have been demonstrated as efficient reducing agents to produce reduced G-O (RG-O). However, some of these reducing agents can introduce additional elements such as nitrogen to the G-O structure. High temperature treatment under a controlled atmosphere is another method to deoxygenate G-O [16–17], but is limited to only substrates that can sustain high temperatures.

Another approach to reduce G-O involves metal (such as Al, Zn, Fe, etc.) powders and foils [18–21]. This route is considered as an efficient and fast method to obtain RG-O without introducing additional elements. In this method, the reduction of G-O occurs due to the hydrogen generated during the reaction of the metal with an acid. The "just generated" hydrogen atoms in these reactions, referred to as 'nascent hydrogen', are transient and highly reactive [22]. It was stated that the G-O dispersions, which are individual G-O platelets suspended in a solution, can be reduced by nascent hydrogen more effectively than by hydrazine [18]. Recently, reduction of G-O films on quartz substrates by nascent hydrogen using remote Al foil immersed in an HCl solution and Zn powder in a NaOH solution has been reported [20]. However, in the G-O films individual G-O platelets are initially fixed on the substrate (not dispersed in the solution), and the nascent

* *Corresponding author.*
E-mail address: r.ruoff@mail.utexas.edu (R.S. Ruoff).
0008-6223/$ - see front matter
http://dx.doi.org/10.1016/j.carbon.2013.07.007

hydrogen was produced remotely from the G-O films, which may diminish the efficiency of reduction. Another challenging issue is that G-O films, deposited onto glass or quartz substrates and immersed into the aqueous solution of HCl or NaOH, can experience partial detachment due to the high dispersibility of G-O in aqueous solutions. This can change the surface morphology and thickness of the G-O films. In the fabrication of RG-O films for TCF applications, where the thickness of RG-O films is only a few nanometers, such detachment of G-O platelets from the substrate may dramatically decrease the performance of the RG-O-based TCFs. In this context, development of reduction methods to fabricate high quality RG-O films is of great importance.

Here, we report the reduction of G-O films directly deposited on Al foil. To avoid the detachment of G-O platelets upon immersion into HCl solution, the G-O film was covered with a thin polymer layer. The nascent hydrogen is generated at the G-O film/Al interface, and effectively reduces the G-O film. Complete etching of the Al foil yields free standing RG-O films that can be transferred onto any target substrate. Transfer of RG-O films onto Ag nanowire films, using the dry transfer method, yielded high-performance hybrid transparent conductive films (TCFs) with opto-electrical properties comparable to that of indium tin oxide (ITO) based TCFs.

2. Experimental

2.1. Synthesis of G-O dispersion

Aqueous G-O dispersions were made by sonication of graphite oxide produced using a modified Hummers' method [11]. Briefly, graphite powder (SP1, Bay Carbon) was oxidized into graphite oxide using sulfuric acid and potassium permanganate. An aqueous dispersion of graphite oxide (1.5 mg/mL) was prepared by sonicating the solid material in pure water (17 MΩ, Barnstead) for 15 min, and then stirring slowly for 10 h.

2.2. Electropolishing of Al foil

Prior to the deposition of G-O films, the Al foil (purchased from Boardwalk, 20 μm thick) used as a substrate for G-O films was electrochemically polished, which results in a smooth surface with a partially removed oxide layer [23]. In the polishing process, Al foil was used as an anode in a two electrode electrochemical cell with an Al plate as cathode. The electrolyte solution composed of 100 mL water, 50 mL ethanol, 10 mL isopropyl alcohol, 50 mL o-phosphoric acid and 1 g urea. A Hewlett-Packard 612 System DC power supply was used to apply a constant potential of 6 V to the electrodes for 10 min. After this electrochemical treatment the Al foil was washed with deionized water and ethanol. A glass substrate (1×1 inch^2), acting, as a rigid support, was attached to the polished Al foil, and the G-O films on the foils were made by spin coating (4000 rpm, 60 s) the aqueous G-O dispersion.

2.3. Preparation of Ag NWs

Ag NWs with lengths of 20–40 μm and diameters of 20–40 nm were synthesized according to the previous report, using a modified polyol method [24]. The as-prepared Ag NWs were then re-dispersed in deionized water (5 mg/mL) with hydroxypropylmethylcellulose (2.5 mg/mL with a dispersing agent (polyethylene glycol sorbitan monolaurate of concentration 0.2 mg/mL) to form an aqueous Ag NW ink. This Ag NW ink was coated on a target substrate using a Meyer rod method, and subsequently dried in an oven at 100 °C for 2 min in ambient atmosphere.

3. Results and discussion

The thicknesses of the G-O films were controlled by varying the concentration of G-O dispersions and spin coating parameters [4]. The G-O films on Al foils were used to produce RG-O films as shown schematically in Fig. 1a. Briefly, G-O films on Al foil (Fig. 1b) were coated with a thin layer of 15 mg/mL poly(methyl methacrylate) (PMMA) (Sigma–Aldrich) dissolved in 99.9% chlorobenzene (Sigma–Aldrich) using spin coating (4000 rpm, 40 s). The PMMA/G-O films on Al foils were heated at 85 °C for 30 min to cure the PMMA. After this process, the Al foils with PMMA/G-O films were detached from the rigid glass support and immersed in 1 M HCl(aq) to dissolve the Al foils. The Al foil vigorously reacted with HCl in the following manner: $2Al + 6HCl \rightarrow 2AlCl_3 + 3H_2$, producing copious amounts of hydrogen. Complete dissolution of the Al foils

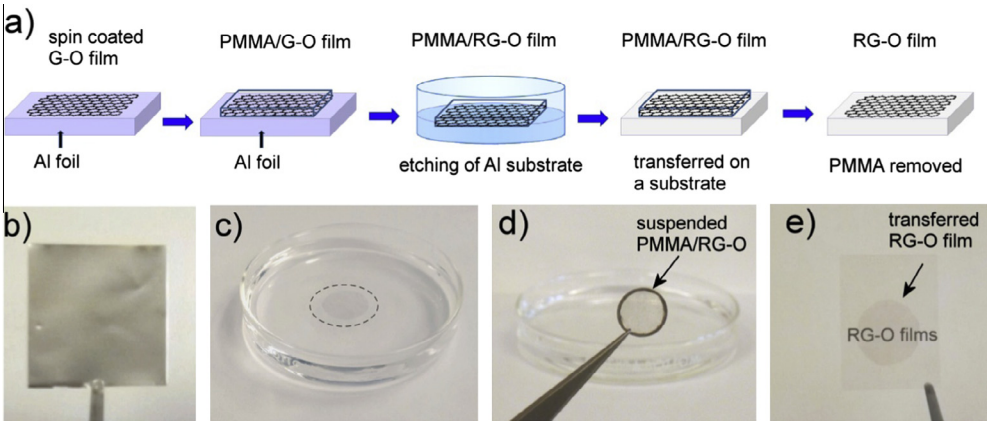

Fig. 1 – (a) Schematic of the reduction of G-O films on Al substrates. Photographs of: (b) G-O films on Al foil, (c) PMMA/RG-O film after etching away the Al foil, (d) free standing PMMA/RG-O film and (e) RG-O film transferred onto a glass substrate.

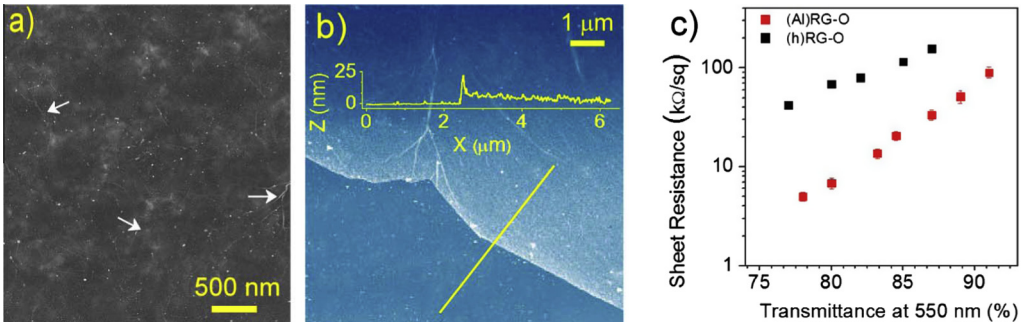

Fig. 2 – (a) Typical SEM and (b) AFM images of (Al)RG-O films transferred onto a SiO_2/Si substrate. White arrows in the SEM image show the edges of (Al)RG-O platelets. (b) AFM image of the Al(RG-O) film transferred onto SiO_2/Si substrate. Line profile corresponding to the yellow line that crosses the film edge is shown. (c) R_s vs T_{550} for the (Al)RG-O films (red squares) and (h)RG-O films (black squares). (For interpretation of the references to colour in this figure legend, the reader is referred to the web version of this article.)

was achieved after about 3 h, yielding RG-O films (Fig. 1c). The PMMA/RG-O films were then washed several times with DI water. Using a rigid metallic ring, the PMMA/RG-O films, floating on the surface of DI water, were 'fished out'. The free standing PMMA/RG-O films (Fig. 1d) were kept at ambient for 2–3 min to completely dry and were then transferred onto target substrates (Fig. 1e). The films were annealed at 100 °C for 1 h in ambient atmosphere, and then kept in desiccators overnight as it was found that this led to better adhesion to the substrate. In the final step, the PMMA was removed using acetone and the RG-O films-on-substrate were annealed at 100 °C for 30 min on a hot plate.

For comparative studies of electrical conductivity, G-O films were also spin coated onto glass substrates (4000 rpm, 60 s) and subsequently reduced by exposure to hydrazine monohydrate (N_2H_4 H_2O, Sigma–Aldrich) vapor at 95 °C. It should be noted that the reduction level in this process depends on the duration of the G-O exposure time to the hydrazine vapor. To compare these films with those reduced by nascent hydrogen, the exposure time was 4 h in our experiments, equivalent to time needed to reduce the G-O films with nascent hydrogen by completely etching the Al foil.

The RG-O films obtained by etching of Al foils are denoted as (Al)RG-O and hydrazine reduced G-O films as (h)RG-O. Fig. 2a shows a typical SEM image of a ~1.8 nm thick (Al)RG-O film transferred onto a SiO_2/Si substrate. The (Al)RG-O platelets form continuous films with smooth surface morphology, similar to that of (h)RG-O films obtained by direct deposition of G-O on a target substrate with subsequent hydrazine reduction [4,10]. No cracks and very few wrinkles or folds were observed in the SEM images. SEM images of the transferred (Al)RG-O films are consistent with the AFM studies shown in Fig. 2b. AFM line profiles show the smooth morphology of the (Al)RG-O film with a thickness of several nanometers.

It is worth noting that the reduction of G-O films and their subsequent delamination from a substrate were reported for G-O films deposited on SiO_2/Si wafer and glass substrates [10,25–26]. The chemical reduction and delamination in these reports were carried out in a two step process that can be time consuming. In contrast, in our work the etching of the Al foil causes the reduction of the G-O film, creating a one step procedure.

Opto-electrical properties of the RG-O films were investigated by measuring the sheet resistance using a four-probe van der Pauw method, and optical transmittance with an ultraviolet–visible-near-infrared (UV–Vis-NIR) spectrometer. The R_s values shown in Fig. 2c were obtained by averaging the R_s of 11–14 samples. Fig. 2c shows that at the same optical transmittance, the (Al)RG-O films have lower sheet resistance than the (h)RG-O films (for example, at T_{550} = 87%, R_s = 35 ± 3.6 kΩ/sq for (Al)RG-O and R_s = 157 ± 10.85 kΩ/sq for (h)RG-O). These results demonstrate that the reduction of G-O films during Al foil etching is more effective compared to the hydrazine reduction process, which is in agreement with the recent reports on reduction of isolated G-O platelets using Al powder in HCl(aq) [18]. In addition, the (Al)RG-O films have noticeably better opto-electrical properties (R_s = 90.13 ± 7.62 kΩ/sq at T_{550} = 91%; and R_s = 20.46 ± 1.95 kΩ/sq at T_{550} = 84.5%) with respect to the RG-O films reduced by similar nascent hydrogen reactions using Al foil in HCl (R_s = 145 kΩ/sq at T_{550} = 91%) and Zn powder in NaOH (R_s = 38.5 kΩ/sq at T_{550} = 84%) [20]. This exhibits the better reduction of G-O films on Al foil, that can be ascribed to higher reduction efficiency of nascent hydrogen generated at the G-O/Al interface.

X-ray photoelectron spectroscopy (XPS) (Kratos photoelectron spectrosocopy system equipped with an Al KR monochromator X-ray source operating at a power of 350 W) was used to analyze the composition of films comprised of G-O, (Al)RG-O, and (h)RG-O. Fig. 3 shows the C 1s XPS spectra of G-O, (Al)RG-O, and (h)RG-O. Deconvolution (by fitting each peak with a combined Gaussian–Lorentzian function after background subtraction) of the C 1s peak in the XPS spectrum of the G-O (Fig. 3a) presents peaks that we assign to C–C (284.5 eV), C–OH (285.7 eV), C–O (286.6 eV), C=O (287.8 eV) and O=C=O (289.1 eV) bonds, [7,11,27] numbered 1–5, respectively. Hydrazine reduction (Fig. 3b) significantly reduces the intensity of the peaks assigned to the C–O, C=O and O–C=O binding energies. In (Al)RG-O films (Fig. 3c) the relative intensity of these peaks is even lower than those for the (h)RG-O films, indicating better reduction in (Al)RG-O films. In addition, the peak at 285.7 eV in the (h)RG-O has larger relative intensity compared to that of the G-O and (Al)RG-O films, which can be ascribed to the incorporation of nitrogen in hydrazine reduced samples (i.e., the peak from the C–N bond

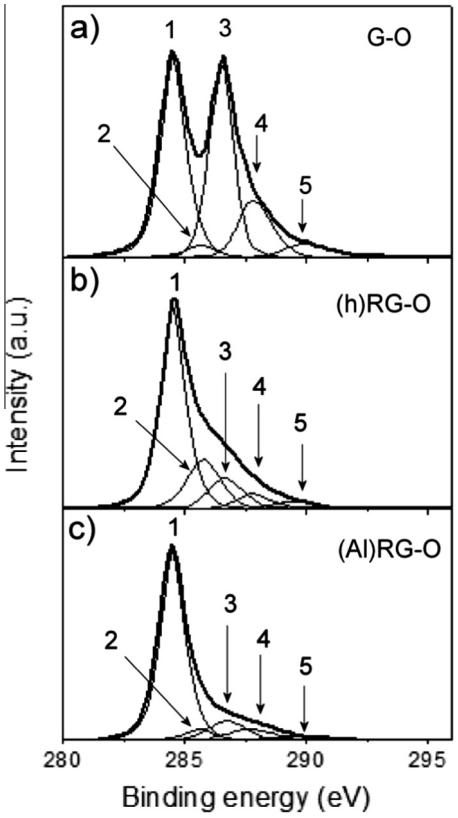

Fig. 3 – C 1s XPS spectra of films of (a) G-O, (b) (h)RG-O, and (c) (Al)RG-O. Deconvolution of the C 1s peak shows the presence of C–C (284.5 eV) – 1; N–C and C–OH (285.7 eV) – 2; C–O (286.6 eV) – 3; C═O (287.8 eV) – 4; and O–C═O (289.1 eV) – 5.

is superimposed on that of the peak due to C–OH bonds) [7,11]. These results agree with data previously reported by other groups [18].

G-O films on Al substrates are mainly reduced by nascent hydrogen produced during etching process of the Al. [18]. Nascent hydrogen, which is transient with a limited lifetime [28], can interact with epoxy, carbonyl and hydroxyl groups of the G-O, producing water molecules and recovering the carbon–carbon bonds [20]. Generation of hydrogen near the G-O/Al interface allows for the immediate interaction between hydrogen and the G-O film, which should efficiently reduce the film. In addition, the high exothermic nature of the reaction between the Al foil and the HCl solution causes an instantaneous increase in the temperature near the G-O/Al interface [29]. This may likely favor the reduction of G-O film, because the efficiency of hydrogen-assisted reduction reactions is higher at elevated temperatures [30]. Additionally, partial reduction of may occur at the G-O/Al interface by electron transfer from Al to G-O because of the high reduction potential for Al/Al^{3+} −1.68 V; for comparison, the reduction potential of hydrazine is –1.16 V) [27]. However, this reduction process has less efficiency compared to that by nascent hydrogen, and it is not the main reduction process [18].

Our recent studies demonstrated that the RG-O can be integrated with metal NW films to produce hybrid TCFs with performance better than the pure metal NW films [4,10]. Here, for fabrication of (Al)RG-O/Ag NW hybrid films, the dry PMMA/RG-O shown in Fig. 1d was transferred onto a Ag NW film. The film was then annealed at 100 °C for 1 h in ambient atmosphere and stored overnight in a desiccators, yielding better adhesion of the (Al)RG-O to the Ag NWs and substrate. Then, the PMMA was removed using acetone and the resulting (Al)RG-O/Ag NW hybrid film was annealed at 100 °C for 30 min on a hot plate. A typical SEM image (Fig. 4a) of the hybrid film shows randomly oriented Ag NWs covered by a continuous (Al)RG-O film. Fig. 4b shows the opto-electrical properties of the hybrid films obtained by assembling the Ag NW films (T_{550} = 97% and R_s = 210 ± 18 Ω/sq) with (Al)RG-O films. In the hybrid films (Al)RG-O layers with T_{550} of 95%, 92%, 87%, and 83% corresponding to average film thicknesses of 0.9, 1.3, 2.1, and 2.7 nm, respectively, were used. (Al)RG-O films lowered the optical transmittance of the hybrid films compared to that of pure Ag NW films. This is due to the fact that in the NW films the optical transmittance is provided by open spaces between NW networks, while in the hybrid films these open spaces are covered by (Al)RG-O, resulting in decreased transmittance. In addition, (Al)RG-O improves the electrical conductivity of the hybrid films. The R_s values shown in Fig. 4b were obtained by averaging the R_s of 8–10 samples. The (Al)RG-O/Ag NW hybrid films with T_{550} = 89% and R_s = 74 ± 7 Ω/sq (Fig. 4b) are comparable to conventional ITO films [31]. The improved electrical conductivity of the hybrid films, compared to pure Ag NW films, is due to the RG-O film that bridges non-contacting Ag NWs [4,10].

Fig. 4c shows the effect of bending on resistance (in the bending direction) for hybrid films deposited on a 300 μm thick poly(ethylene terephthalate) (PET) substrate (inset in Fig. 4c). The bending experiments were carried out using a two-probe electrical contact equipment and a precision mechanical system. For these experiments we prepared hybrid films with dimensions of 30 × 10 mm^2. Two silver wires, used to measure the resistance of the samples, were connected to two short edges (far from the central area) of the samples using silver paste. During the measurements, the central area of the samples was bent while the areas with electrodes were unchanged. The thickness of the percolated Ag NWs films in our samples is ~100 nm, and therefore, the thickness of the PET alone was used to calculate the tensile strain shown in Fig. 4c. No significant changes (<7%) in resistance were observed for films bent up to a curvature radius of ⩾5 mm (tensile strain ⩽3%). Further decrease of the bending radius resulted in a gradual increase in resistance. When the bending radius was decreased to 2.5 mm (tensile strain = 6%) the film resistance almost doubled (from 90 Ω to 172 Ω). The film resistance returned to the initial value after flattening the film even after 100 bending cycles, demonstrating 'good' mechanical stability of the film, similar to that of pure Ag NW [24] or RG-O films [25,32].

In recent reports, RG-O/Ag NW hybrid films have been obtained by spin coating G-O dispersions onto Ag NW films, and the G-O/Ag NW hybrid film was subsequently reduced with hydrazine [4]. In this method, the spin coating of G-O films on top of the Ag NW films may result in the significant modifications to the initial film structure of the NWs, and may adversely affect the performance of the final hybrid films. In addition, the nascent hydrogen reduction method using remote Al etching,

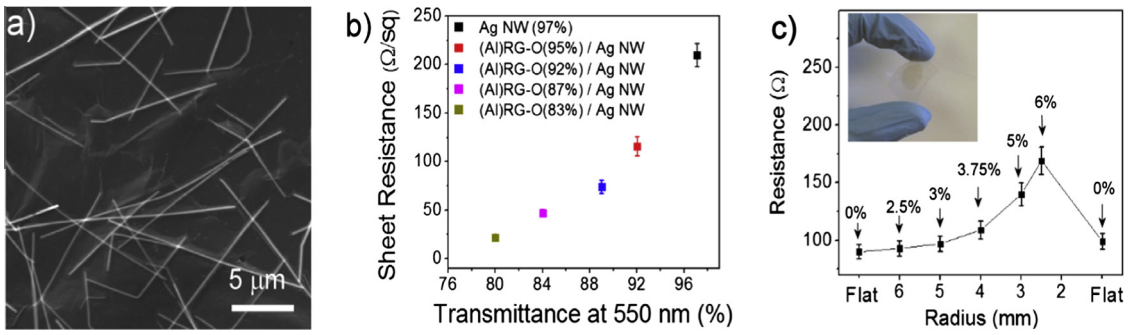

Fig. 4 – (a) SEM image of (Al)RG-O/Ag NW hybrid films. (b) R_s vs T_{550} of a pure Ag NW film (T_{550} = 97% and R_s = 210 ± 18 Ω/sq), and its hybrids with (Al)RG-O films (T_{550} shown in parentheses). (c) Changes in R_s during the bending of the substrate. Tensile strain (in%) values are shown for corresponding bending radius. Inset shows the photograph of the (Al) RG-O/Ag NW hybrid film on a flexible PET substrate.

as reported in [20], cannot be directly used to reduce G-O/Ag NW hybrid films deposited on quartz or glass substrates because of the strong interactions between Ag NWs and the HCl solution. Our method presented in this work allows for the simultaneous high-efficiency reduction and fabrication of free standing RG-O films that can be transferred onto metal NW films without influencing their initial structural characteristics. These features of our method demonstrate its advantage over the previously reported approaches for the fabrication of hybrid RG-O/metal NW hybrid TCFs.

4. Summary

G-O films deposited on Al foil were reduced with nascent hydrogen generated by immersing the Al foil in HCl (aq). Complete etching of Al foils yield free standing RG-O films. Such RG-O films have better electrical conductivity compared to those obtained by exposure to hydrazine or reduced by nascent hydrogen using remote Al foil in HCl solution. Dry transfer of such (Al)RG-O films onto Ag NW films yields hybrid TCFs with optical and electrical properties comparable to ITO films. Simultaneous reduction of G-O films and the generation of free-standing RG-O films combined with the dry transfer method are an attractive route for fabrication of large-area RG-O-based thin films and coatings for diverse applications.

Acknowledgements

This work was supported by National Science Foundation (Grant #: DMR-1206986). A.J.G.Z. and S.H.D. Gratefully acknowledge the CNPq, INCT of Carbon Nanomaterials (CNPq), NENNAM (Pronex F. Araucária/CNPq), and CAPES for the financial support.

REFERENCES

[1] Stankovich S, Dikin DA, Dommett GHB, Kohlhaas KM, Zimney EJ, Stach EA, et al. Graphene-based composite materials. Nature 2006;442(7100):282–6.
[2] Kim J-Y, Lee WH, Suk JW, Potts JR, Chou H, Kholmanov IN, et al. Chlorination of reduced graphene oxide enhances the dielectric constant of reduced graphene oxide/polymer composites. Adv Mater 2013;25(16):2308–13.
[3] Dikin DA, Stankovich S, Zimney EJ, Piner RD, Dommett GHB, Evmenenko G, et al. Preparation and characterization of graphene oxide paper. Nature 2007;448(7152):457–60.
[4] Kholmanov IN, Stoller MD, Edgeworth J, Lee WH, Li H, Lee J, et al. Nanostructured hybrid transparent conductive films with antibacterial properties. ACS Nano 2012;6(6):5157–63.
[5] Wu J, Agrawal M, Becerril HA, Bao Z, Liu Z, Chen Y, et al. Organic light-emitting diodes on solution-processed graphene transparent electrodes. ACS Nano 2009;4(1):43–8.
[6] Moon IK, Kim JI, Lee H, Hur K, Kim WC, Lee H. 2D Graphene oxide nanosheets as an adhesive over-coating layer for flexible transparent conductive electrodes. Sci Rep 2013;3.
[7] Becerril HA, Mao J, Liu Z, Stoltenberg RM, Bao Z, Chen Y. Evaluation of solution-processed reduced graphene oxide films as transparent conductors. ACS Nano 2008;2(3):463–70.
[8] Eda G, Chhowalla M. Chemically derived graphene oxide: towards large-area thin-film electronics and optoelectronics. Adv Mater 2010;22(22):2392–415.
[9] Schwamb T, Burg BR, Schirmer NC, Poulikakos D. An electrical method for the measurement of the thermal and electrical conductivity of reduced graphene oxide nanostructures. Nanotechnology 2009;20(40):405704.
[10] Kholmanov IN, Domingues SH, Chou H, Wang X, Tan C, Kim J-Y, et al. Reduced graphene oxide/copper nanowire hybrid films as high-performance transparent electrodes. ACS Nano 2013;7(2):1811–6.
[11] Stankovich S, Dikin DA, Piner RD, Kohlhaas KA, Kleinhammes A, Jia Y, et al. Synthesis of graphene-based nanosheets via chemical reduction of exfoliated graphite oxide. Carbon 2007;45(7):1558–65.
[12] Si Y, Samulski ET. Synthesis of water soluble graphene. Nano Lett 2008;8(6):1679–82.
[13] Wang G, Yang J, Park J, Gou X, Wang B, Liu H, et al. Facile synthesis and characterization of graphene nanosheets. J Phys Chem C 2008;112(22):8192–5.
[14] Moon IK, Lee J, Lee H. Highly qualified reduced graphene oxides: the best chemical reduction. Chem Commun 2011;47(34):9681–3.
[15] Zhang J, Yang H, Shen G, Cheng P, Zhang J, Guo S. Reduction of graphene oxide vial-ascorbic acid. Chem Commun 2010;46(7):1112–4.
[16] Dreyer DR, Park S, Bielawski CW, Ruoff RS. The chemistry of graphene oxide. Chem Soc Rev 2010;39(1):228–40.
[17] Gong C, Acik M, Abolfath RM, Chabal Y, Cho K. Graphitization of graphene oxide with ethanol during thermal reduction. J Phys Chem C 2012;116(18):9969–79.

[18] Fan Z, Wang K, Wei T, Yan J, Song L, Shao B. An environmentally friendly and efficient route for the reduction of graphene oxide by aluminum powder. Carbon 2010;48(5):1686–9.
[19] Wan D, Yang C, Lin T, Tang Y, Zhou M, Zhong Y, et al. Low-temperature aluminum reduction of graphene oxide, electrical properties, surface wettability, and energy storage applications. ACS Nano 2012;6(10):9068–78.
[20] Pham VH, Pham HD, Dang TT, Hur SH, Kim EJ, Kong BS, et al. Chemical reduction of an aqueous suspension of graphene oxide by nascent hydrogen. J Mater Chem 2012;22(21):10530–6.
[21] Fan Z-J, Kai W, Yan J, Wei T, Zhi L-J, Feng J, et al. Facile synthesis of graphene nanosheets via Fe reduction of exfoliated graphite oxide. ACS Nano 2010;5(1):191–8.
[22] Laborda F, Bolea E, Baranguan MT, Castillo JR. Hydride generation in analytical chemistry and nascent hydrogen: when is it going to be over? Spectrochim Acta B 2002;57(4):797–802.
[23] Zhang B, Lee WH, Piner R, Kholmanov I, Wu Y, Li H, et al. Low-temperature chemical vapor deposition growth of graphene from toluene on electropolished copper foils. ACS Nano 2012;6(3):2471–6.
[24] Kim T, Kim YW, Lee HS, Kim H, Yang WS, Suh KS. Uniformly interconnected silver-nanowire networks for transparent film heaters. Adv Funct Mater 2013;23(10):1250–5.
[25] Yamaguchi H, Eda G, Mattevi C, Kim H, Chhowalla M. Highly uniform 300 mm wafer-scale deposition of single and multilayered chemically derived graphene thin films. ACS Nano 2010;4(1):524–8.
[26] Kang D, Kwon JY, Cho H, Sim J-H, Hwang HS, Kim CS, et al. Oxidation resistance of iron and copper foils coated with reduced graphene oxide multilayers. ACS Nano 2012;6(9):7763–9.
[27] Liu Q, He M, Xu X, Zhang L, Yu J. Self-assembly of graphene oxide on the surface of aluminum foil. New J Chem 2013;37(1):181–7.
[28] Fuentes-Aceituno JC, Lapidus GT, Doyle FM. A kinetic study of the electro-assisted reduction of chalcopyrite. Hydrometallurgy 2008;92(1–2):26–33.
[29] Coughlin JP. Heats of formation and hydration of anhydrous aluminum chloride. J Phys Chem 1958;62(4):419–21.
[30] Salvatierra RV, Domingues SH, Oliveira MM, Zarbin AJG. Tri-layer graphene films produced by mechanochemical exfoliation of graphite. Carbon 2013;57:410–5.
[31] Tahar RBH, Ban T, Ohya Y, Takahashi Y. Tin doped indium oxide thin films: electrical properties. J Appl Phys 1998;83(5):2631–45.
[32] Eda G, Fanchini G, Chhowalla M. Large-area ultrathin films of reduced graphene oxide as a transparent and flexible electronic material. Nat Nanotechnol 2008;3(5):270–4.